Silver Nanoparticle and Nanowire Formation by Microtubule Templates

Silke Behrens,*,† Jin Wu,†,‡ Wilhelm Habicht,† and Eberhard Unger§

Institut für Technische Chemie, Forschungszentrum Karlsruhe, Postfach 3640, D-76021 Karlsruhe, Institut für Molekulare Biotechnologie, Postfach 100813, D-07708 Jena, Germany, and Department of Chemistry, Graduate School of Chinese Academy of Sciences, Beijing 100039, P. R. China

Received March 31, 2004. Revised Manuscript Received May 19, 2004

The synthesis of increasingly miniaturized structures using alternative techniques is strongly motivated by future applications in areas such as nanoelectronics. Highly ordered protein assemblies of tubular structure and high geometric aspect ratio are used as bioorganic templates for the bottom-up synthesis of metal nanostructures. When the biotemplate is coupled to an appropriate chemical reaction, metal is generated in situ and deposited along the backbone of the biostructure. Ag/protein structures with different morphologies are produced, from microtubules densely covered with small Ag nanoparticles to continuous Ag nanowires. Our results demonstrate the potential of bioassemblies in general for the fabrication of multidimensional structures with interesting material properties.

1. Introduction

Commercial requirements to produce increasingly miniaturized structures, e.g., as components for microelectronic devices, strongly motivates the synthesis of nanoscale systems using alternative techniques. Biomolecular structures have typical size dimensions from the lower nanometer size range up to several micrometers together with well-defined surface functionalities. Because of their molecular recognition capabilities, many among them are able to self-assemble into complex, well-defined, and extended superstructures. However, concerning intrinsic electric conductivity, for example, biological systems often do not exhibit the desired physical properties. Recently, biological systems have been explored as building blocks in the bottom-up assembly and generation of new inorganic materials and devices with advanced structures and functionalities.[1−3] For example, well-defined nanoparticles have been synthesized by the mineralization of proteins[4] and viruses.[5−8] The specific recognition properties of oligonucleotides[9,10] and antibodies[11] have been used to generate three-dimensional well-ordered aggregates of metal nanoparticles. Motivated by future applications in nanoelectronics, researchers have employed DNA strands to create conductive silver,[12−14] palladium,[15] platinum,[16,17] or copper[18] nanowires. Furthermore, self-assembled systems such as lipid tubules have been used as metallization templates.[19,20] Other wet chemical strategies in aqueous solutions have involved the seed-mediated growth of silver nanowires in the presence of a surfactant,[21] growth of silver nanowires with sodium citrate and sodium hydroxide,[22] or growth of silver nanowires in the pores of self-assembled calix[4]-hydroquinone nanotubes.[23]

Here, we show how microtubules can be used as a template for the formation of spherical silver nanoparticles as well as continuously covered silver nanowires.

Microtubules are proteinaceous cylindrical structures, found in nearly all eukaryotes.[24] As part of the cytoskeleton, they are involved in essential life processes including mitosis, maintenance of cell shape, cell motility, and intracellular transport of organelles. In vitro,

* Corresponding author. E-mail: silke.behrens@itc-cpv.fzk.de. Phone: +49-(0)7247-826512. Fax: +49-(0)7247-822244

† Forschungszentrum Karlsruhe.

‡ Graduate School of Chinese Academy of Sciences.

§ Institut für Molekulare Biotechnologie.

(1) Dujardin, E.; Mann, S. *Adv. Mater.* **2002**, *14*, 775.
(2) Niemeyer, C. M. *Angew. Chem., Int. Ed.* **2001**, *40*, 4129.
(3) Storhoff, J.; Mirkin, C. *Chem. Rev.* **1999**, *99*, 1849.
(4) Wong, K.; Mann, S. *Adv. Mater.* **1996**, *8*, 929.
(5) Shenton, W.; Douglas, T.; Young, M.; Stubbs, G.; Mann, S. *Adv. Mater.* **1999**, *11*, 253.
(6) Dujardin, E.; Peet, C.; Stubbs, G.; Cluver, J.; Mann, S. *Nano Lett.* **2003**, *3*, 413.
(7) Knez, M.; Bittner, A. M.; Boes, F.; Wege, C.; Jeske, H.; Maiss, E.; Kern, K. *Nano Lett.* **2003**, *8*, 1079.
(8) Douglas, T.; Young, M. *Nature* **1998**, *393*, 152.
(9) Mirkin, C.; Letsinger, R.; Mucic, R.; Storhoff, J. *Nature* **1996**, *382*, 607.
(10) Cao, Y.; Jin, R.; Mirkin, C. *J. Am. Chem. Soc.* **2001**, *123*, 7961.
(11) Connolly, S.; Fitzmaurice, D. *Adv. Mater.* **1999**, *11*, 1202.
(12) Braun, E.; Eichen, Y.; Sivan, U.; Ben-Yoseph, G. *Nature* **1998**, *391*, 775.
(13) Keren, K.; Krueger, M.; Gilad, R.; Ben-Yoseph, G.; Sivan, U.; Braun, E. *Science* **2002**, *297*, 72.
(14) Keren, K.; Berman, R.; Braun, E. *Nano Lett.* **2004**, *4*, 323.
(15) Richter, J.; Mertig, M.; Pompe, W. *Appl. Phys. Lett.* **2001**, *78*, 536.
(16) Ford, W.; Harnack, O.; Yasuda, A.; Wessels, J. *Adv. Mater.* **2001**, *13*, 1793.
(17) Mertig, M.; Ciacchi, L. C.; Seidel, R.; Pompe, W.; De Vita, A. *Nano Lett.* **2002**, *2*, 841.
(18) Monson, C.; Woolley, A. *Nano Lett.* **2003**, *3*, 359.
(19) Markowitz, M.; Baral, S.; Brandow, S.; Singh, A. *Thin Solid Films* **1993**, *224*, 242.
(20) Kogiso, M.; Yoshida, K.; Yase, K.; Shimizu, T. *Chem. Commun.* **2002**, 2492.
(21) Murphy, C.; Jana, N. *Adv. Mater.* **2002**, *14*, 80.
(22) Caswell, K.; Bender, C.; Murphy, C. *Nano Lett.* **2003**, *3*, 667.
(23) Hong, B. H.; Bae, S. C.; Lee, C. W.; Jeong, S.; Kim, K. S. *Science* **2001**, *294*, 348.
(24) Nogales, E. *Annu. Rev. Biochem.* **2000**, *69*, 277.

10.1021/cm049462s CCC: $27.50
Published on Web 07/09/2004

microtubules can be assembled from tubulin at physiological pH, ionic strength, and temperature in the presence of the cofactors Mg^{2+} and guanosine-5′-triphosphate (GTP). A microtubule is formed by a more or less parallel association of protofilaments, composed of α,β-tubulin subunits with a strict α, β alternation. The length of the tubulin dimer is about 8 nm, and its diameter is 4−5 nm. Depending on the assembly conditions in vitro, 13−14 protofilaments are longitudinally aligned to a cylindrical structure with an outer diameter of 25 nm and lengths of several micrometers. Interestingly, tubulin is able to form not only microtubules but also numerous polymorphic assemblies, among them sheets, spirals, ribbons, and rings.[25]

Tubulin molecules consist of chemically functional surfaces with defined patterns of amino acid side chains that provide a wide variety of active sites for the nucleation, organization, and binding of metal particles. These properties of microtubules have been exploited for the template-directed nucleation of palladium[26] and gold[27] nanoparticles. The preferential and very regular deposition of nanoparticles observed in the presence of the biopolymer suggested that defined interactions between the functional groups of the protein surface and the palladium in solution were important during particle nucleation. Using electroless metal plating techniques, nickel and cobalt were deposited on the biostructure.[28,29] Recently, the microtubule-templated biomimetic mineralization of iron oxide has been described.[30]

2. Experimental Section

Materials. Ethylene glycol bis(2-aminoethyl ether) tetraacetic acid (EGTA), 1,4-piperazine diethane sulfonic acid (PIPES), guanosine-5′-triphosphate lithium salt, taxol, glutaric dialdehyde, silver nitrate, and hydroquinone were purchased from Sigma-Aldrich. Nanopure water (18.2 ΩM) prepared with a Milli-Q Plus water system was used throughout the experiments.

Microtubule Assembly. Microtubule protein was purified from porcine brain by an in vitro assembly−disassembly process. The final protein concentration was about 1 mg mL^{-1}. The microtubules were assembled in vitro in a buffer solution of 20 mM PIPES (pH 6.8), 80 mM $NaNO_3$, 0.5 mM $Mg(NO_3)_2$, and 1 mM EGTA by adding 0.25 M GTP and, after 20 min, 10 mM taxol (from *Taxus brevifolia*) and warming the sample to 37 °C. The microtubule formation was followed by turbidity measurements at $\lambda = 360$ nm and controlled by electron microscopy. The steady-state level at which the tubulin mass in the polymerized state showed no further increase was usually observed ca. 5 min after taxol addition.

The assembled microtubules were chemically fixed in 0.1% glutaric dialdehyde. The samples were finally dialyzed against PIPES buffer (diluted 10-fold with H_2O) to eliminate excess glutaric dialdehyde.

Synthesis of Silver Nanoparticles with $NaBH_4$. A 600-μL portion of an aqueous $AgNO_3$ solution (1 mM) was added to 60 μL of microtubule suspension (fixed with glutaric dialdehyde, see above) and reduced by rapidly adding 180 μL of an aqueous $NaBH_4$ solution (2.5 mM) at 0 °C.

The resulting microtubule-bound silver nanoparticles could be further developed with 240 μL of hydroquinone solution (0.05 M in water) and 360 μL of $AgNO_3$ solution (5 mM in water).

Synthesis of Silver Nanowires. A 60-μL sample of assembled microtubules (fixed with glutaric dialdehyde, see above) was diluted to 630 μL with PIPES buffer. The protein assemblies were then incubated with 30 μL of an aqueous $AgNO_3$ solution (0.1 M) for 2 h at room temperature in the dark. In a second step, 240 μL of a reduction bath containing hydroquinone (0.05 M in water) was added. The reaction was typically stopped by adding an excess of $Na_2S_2O_3$ (120 μL of a 0.25 M solution in water) after 1, 2.5, or 7 min or by adsorption of the sample on a TEM grid. When the diluted microtubules were incubated with only 10 μL of the aqueous $AgNO_3$ solution, large silver aggregates were attached to the microtubules, and no continuous silver coating was observed.

Electron Microscopy. TEM observations of decorated microtubules were made with a Philips Tecnai F20 TEM with field emission gun at 200 kV; SEM observations were made with a LEO Gemini 982 SEM equipped with a LINK ISIS 300 EDX analysis unit from Oxford Corp. Typically, a 20-μL droplet of the sample was placed on a carbon-coated 400-mesh copper grid, and the excess liquid was removed with a filter paper. When negative staining was performed, the dried sample on the TEM grid was additionally exposed to a 1% uranyl acetate solution for ca. 1 min. For TEM investigations, metallized microtubules were sedimented at 20 000*g*, embedded in Vestopal W, ultrathin sectioned, and mounted on slot grids.

UV−Visible Spectroscopy. UV−visible absorption spectra were recorded in a 1400-μL quartz cuvette (10-mm path length) on a Zeiss MCS 501 UV−NIR spectrometer. The reactions were started by rapidly adding the reducing agent directly into the cuvette. For reduction of Ag^+/MT mixtures with $NaBH_4$, data were collected every 15 s for 5 min for a 700-μL sample in the 270−800 nm range at 0 °C. For baseline subtraction, the spectra were recorded against a buffer/microtubule/$AgNO_3$ reference.

3. Results and Discussion

Because of their cellular functions, microtubules are highly dynamic structures that permanently polymerize and depolymerize even at the assembly disassembly steady state.[31,32] Using glutaric dialdehyde, we cross-linked the tubulin subunits and thus suppressed the dynamic properties of the polymer. This treatment stabilizes the microtubule filament toward thermal and chemical treatments, such as cooling and deviations from physiological pH.

Glutaric dialdehyde-stabilized microtubules were incubated with $AgNO_3$ for ca. 1 min at 0 °C, and then sodium borohydride as a reducing agent was rapidly added. Figure 1 shows microtubules with a dense coating of discrete silver nanoparticles, 5.2 nm in size, across the entire surface of the biopolymer.

The reduction of silver ions by sodium borohydride yielded small spherical silver nanoparticles that were attached to the microtubule surface. Under these conditions, the particles were bound to the surface of the biotemplate for the most part, and only a few unattached particles were observed by TEM. When the silver ions were reduced with sodium borohydride under the same conditions but without any microtubule template present, no nanoparticles were obtained; instead,

(25) Unger, E.; Vater, W.; Böhm, K.-J. *Electron Microsc. Rev.* **1990**, *3*, 355.
(26) Behrens, S.; Rahn, K.; Habicht, W.; Böhm, K. J.; Rösner, H.; Dinjus, E.; Unger, E. *Adv. Mater.* **2002**, *22*, 1621.
(27) Behrens, S.; Unger, E. In *Dekker Encyclopedia of Nanoscience and Nanotechnology*; Schwarz, J., Contescu, C., Putyera, K., Eds.; Marcel Dekker: New York, 2004; pp 2563−2570.
(28) Kirsch, R.; Mertig, M.; Pompe, W.; Wahl, R.; Sadowski, G.; Böhm, K.-J.; Unger, E. *Thin Solid Films* **1997**, *305*, 248.
(29) Mertig, M.; Kirsch, R.; Pompe, W. *Appl. Phys. A 66* **1998**, 723.
(30) Boal, A. K.; Headley, T. J.; Tissot, R. G.; Bunker, B. C. *Adv. Funct. Mater.* **2004**, *14*, 19.
(31) Roth, J. *Histochem. Cell. Biol.* **1996**, *106*, 1.
(32) Oliver, C. *Methods Mol. Biol.* **1999**, *115*, 331.

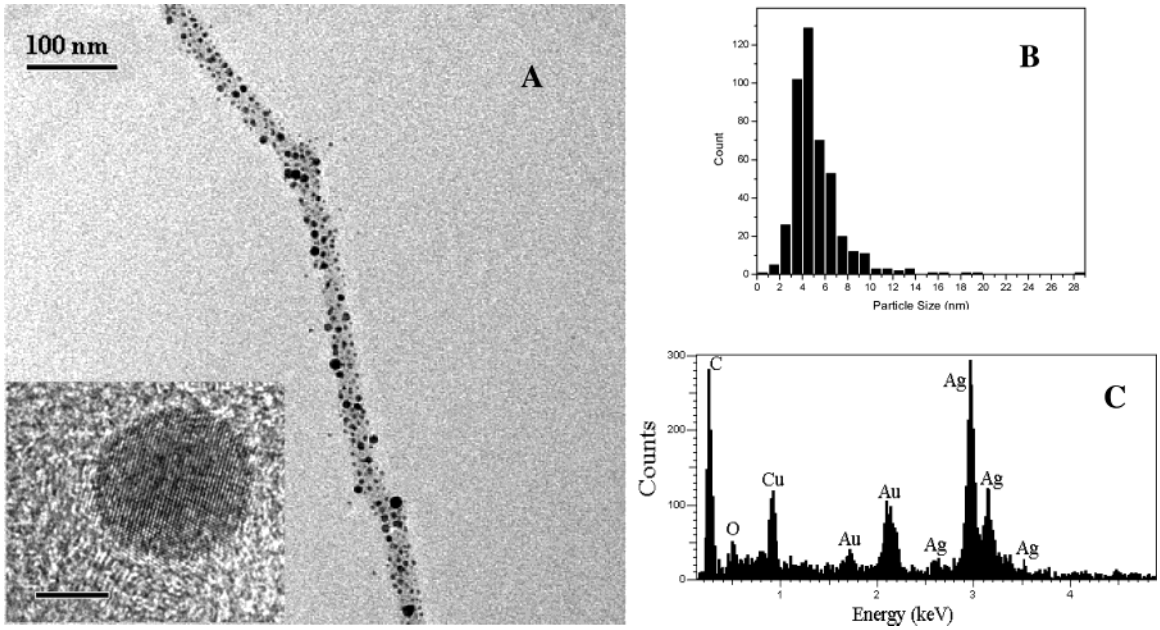

Figure 1. (A) TEM micrograph showing microtubules densely covered by ~5.2-nm silver nanoparticles (scale bar = 100 nm). Inset: HRTEM image showing a silver particle bound to a microtubule (scale bar = 5 nm). (B) Particle size distribution of microtubule-supported silver particles as obtained from TEM images (mean particle diameter = 5.2 ± 2.5 nm). (C) EDX spectrum of the metallized microtubule showing the presence of silver. Grid holder, Au; supporting TEM grid, Cu.

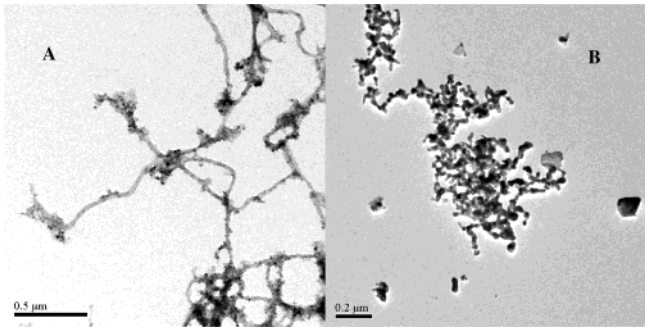

Figure 2. Reduction of silver nitrate with sodium borohydride (A) in the presence of microtubules and (B) without microtubules. The filamentous projections from the microtubule surface seen in A are most probably due to microtubule-associated proteins (MAPs).

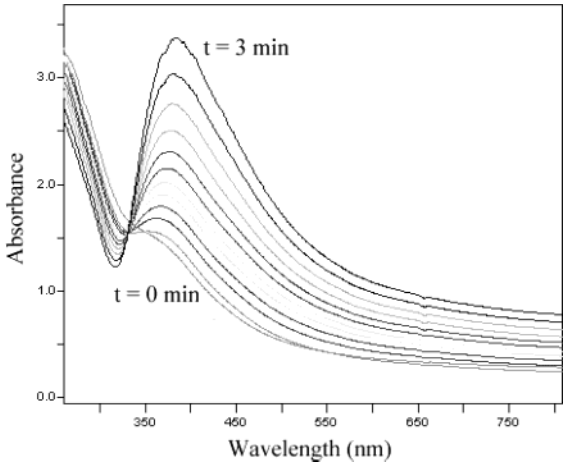

Figure 3. Evolution of UV−visible absorption for silver particles obtained by reduction with sodium borohydride in the presence of microtubules at 0 °C. The interval between the spectra is 15 s. The absorption spectra display a plasmon band, characteristic of metallic silver colloids, occurring a few seconds after the addition of sodium borohydride.

large Ag agglomerates were finally formed in the solution (Figure 2). These observations suggest that the microtubule template is important for nucleation and stabilization of the silver particles.

Lattice *d* spacings of 0.23 nm (111), 0.20 nm (200), and 0.14 nm (220) measured from selected-area electron diffraction (SAED) patterns suggest that the particles were crystallized in the face-centered-cubic (fcc) structure of a metallic silver phase. Figure 1 displays a typical high-resolution TEM (HRTEM) image of an individual silver particle bound to a microtubule. The well-resolved interference fringe patterns confirmed the crystallinity of the silver particles. In addition, the purity of Ag particles was demonstrated by energy-dispersive X-ray analysis (EDX) (Figure 1).

Conceptually, particle formation could involve two mechanisms: (1) formation of conjugates between silver seeds homogeneously nucleated in solution and the microtubule template or (2) heterogeneous nucleation of silver particles on the microtubule surface after adsorption of silver ions onto the functionalities of the biotemplate. When the incubation time of the template with the silver ions was increased from 1 min to 2 h, the observed particles grew only slightly in size (about 0.9 nm), whereas the particle densities on the substrate seemed to be similar in both cases. In the case of the reducing agent being added to the template prior to the metal ions, larger silver particles (ca. 9 nm in size) were observed on the microtubule surface. On the basis of these observations, particle nucleation could occur homogeneously in solution as well as heterogeneously on the biotemplate. During reduction of silver ions with sodium borohydride, each of the two mechanisms probably contributes partially to the decoration of microtubules with silver nanoparticles. In general, the affinity of silver ions to amino acids depends to a large extend on the amino acid side chain.[33] Potential sites for the binding of silver ions and heterogeneous silver nucle-

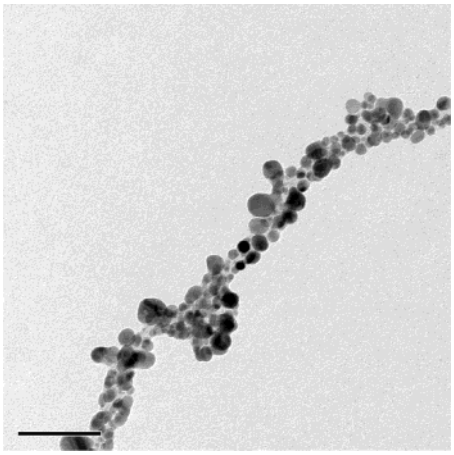

Figure 4. TEM image of a microtubule densely covered by silver grains, 10 to 30 nm in size, obtained upon developing the nucleated silver nanoparticles with hydroquinone and silver ions (scale bar = 100 nm).

ation could be nitrogen-containing side chains of the amino acids. For example, histidines are situated freely accessible at the outside wall of microtubules,[26] although they are protonated at pH 6, which would exclude them as N donor ligands below this pH value. Conjugation of homogeneously nucleated silver particles to the template could involve interactions such as electrostatic forces between positively charged domains at the microtubule surface or van der Waals forces. It has been suggested that borohydride ions adsorb to the surface of silver particles, thus providing a negatively charged particle surface.[34] Even at pH values above the isoelectric point (about pH 4.2[35]) and a net negative surface charge, microtubules display on their surface negatively and positively charged as well as neutral domains, with the positively charged domains gaining more and more importance with decreasing pH, thus giving rise to an increasing binding tendency for the negatively charged particles. This could explain why the decoration of microtubules with silver particles is poor for pH values above 7.

The process of particle formation was followed by UV−visible absorption spectra. Spectra were recorded every 15 s at 0 °C on a Zeiss MCS 501 UV−NIR spectrometer. Figure 3 shows the evolution of the UV−visible absorbance for a silver/microtubule solution reacted with sodium borohydride.

The absorption spectra display a plasmon band, which is characteristic of metallic silver colloids,[34] occurring a few seconds after the addition of sodium borohydride. The plasmon peak is originally centered at ∼370 nm and then red shifts to ∼400 nm after 5 min. Initially, a rapid increase of the plasmon peak was observed; later, the peak grew more slowly in magnitude, which suggests the depletion of reactants.

The obtained silver particles can be further "developed" using an aqueous solution of hydroquinone and silver ions under low light conditions. This reaction has been widely studied in connection with photographic procedures.[36] When this strategy was employed, the microtubule-bound silver aggregates acted as a catalyst for further particle growth that resulted in metal

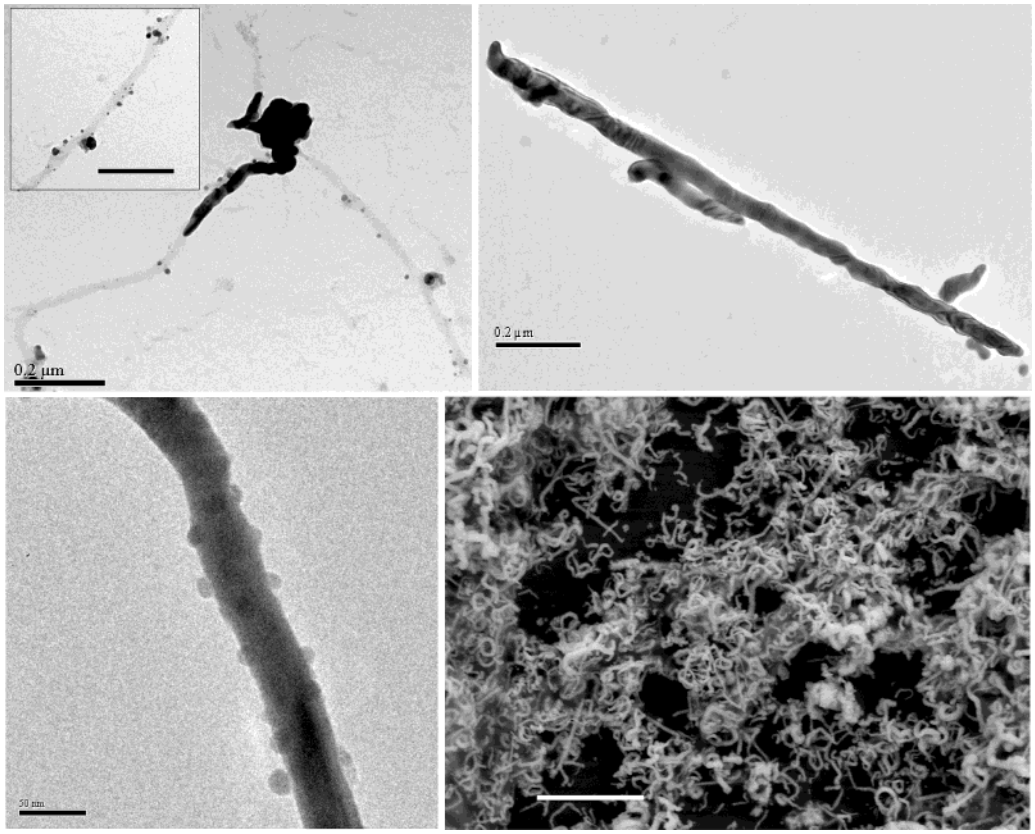

Figure 5. (A) TEM image of microtubules partially covered by a silver coating and small silver seeds obtained by hydroquinone reduction of silver nitrate (scale bar = 0.2 μm). Inset: Microtubule covered by small silver nuclei (scale bar = 0.2 μm). (B) and (C) TEM images of microtubules continuously covered by a silver coating (B, scale bar = 200 nm; C, scale bar = 50 nm). (D) SEM micrograph of a network consisting of several silver nanowires taken with a secondary electron in-lens detector (10 kV, scale bar = 2 μm).

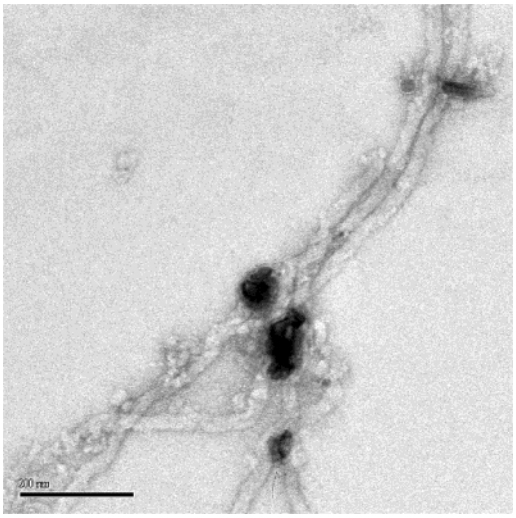

Figure 6. TEM micrograph of microtubules treated with a low silver concentration followed by hydroquinone reduction (negatively stained with 1% uranyl acetate solution; scale bar = 0.2 μm). The light gray lines indicate stained microtubules; the dark spots are silver aggregates.

deposition mainly along the microtubule backbone. The obtained wire consisted of enlarged silver grains of 10−30 nm deposited along the microtubule skeleton. Figure 4 shows a TEM image of a microtubule densely covered by silver grains obtained by this "development" procedure.

In addition to this development procedure, direct reduction of silver ions with hydroquinone in the presence of microtubule templates was possible. In this case, microtubules were incubated with silver nitrate for 2 h at room temperature in the dark, and hydroquinone was then added rapidly. After ca. 2−3 min, the reaction mixture turned black, indicating reduction of silver ions and formation of metallic silver wires. By adding an excess of $S_2O_3^{2-}$ to the reaction mixture, the reduction process could be stopped at any time, forming thiosulfate complexes with unreduced silver ions in solution. Shortly after the addition of hydroquinone (after ca. 1 min of reaction), small silver nuclei appeared on the biotemplate. After ca. 2−2.5 min, the microtubules were mainly covered by a silver coating; however, parts still remained that were covered by small silver nuclei. Figure 5A shows such a microtubule covered partially by a silver film and partially by remaining silver nuclei. Whereas the development procedure resulted only in discontinuous silver coating of the microtubules with some gaps between the large silver grains, the above procedure yielded microtubules that appeared to be mainly covered by a continuous silver coating. TEM images of such silver nanowires (obtained after a 2.5-min reaction time) are displayed in Figure 5B and 5C. The mean diameter of the silver wires measured from the TEM images after 2.5 min of reaction was 39.6 ± 2 nm, and it grew to 76.8 ± 2.6 nm after 7 min. The obtained solutions were found to be unstable because of the agglomeration of the wires into extended networks, which resulted in a fine black precipitate usually settling after several minutes (Figure 5D).

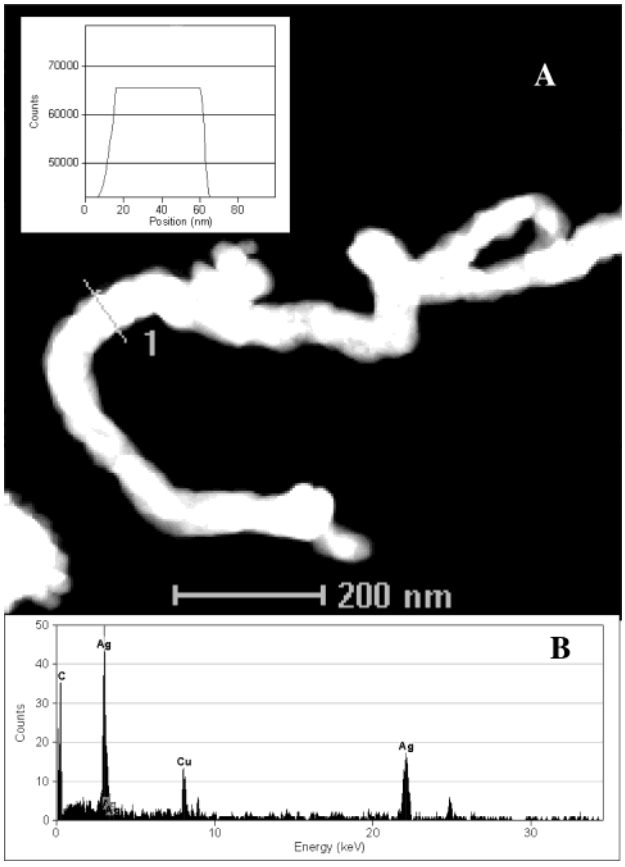

Figure 7. (A) High-angle annular-darkfield (HAAD) scanning transmission electron micrograph showing silver-metallized microtubules resulting from hydroquinone reduction after 7 min. The inset shows the EDX (Ag $K_{\alpha 1}$) linescan in 1. (B) EDX spectrum of a continuous silver nanowire showing the presence of silver. Supporting TEM grid, Cu.

The obtained product was sensitively dependent on the reaction conditions applied. For example, when the microtubules (0.06 mg) were treated with lower quantities of silver ions (1×10^{-6} mol Ag^+ instead of 3×10^{-6} mol Ag^+), only large silver aggregates attached to microtubules and no continuous wires were observed.

TEM images of the negatively stained samples revealed that silver deposition occurred mainly at the surface of the protein assembly (Figure 6), although some excess particles were also detected in the background of the grid. The light gray lines shown in Figure 6 represent stained microtubules that are obviously not covered by silver; the dark spots are silver aggregates.

Corresponding SAED patterns of the silver wires showed lattice *d* spacings at 0.23, 0.20, and 0.14 nm, which were consistent with the (111), (200), and (220) planes of the fcc structure of a pure metallic silver phase. The crystalline character of the nanowires was also demonstrated by HRTEM images, which showed clearly resolved lattice fringes. Despite the general crystallinity of the nanowires, the results indicated that each silver-metallized microtubule was not a single crystal, but polycrystalline. A further confirmation of the silver nanorods was obtained from the energy-dispersive spectrometer in the TEM, which showed that the particles were made of silver (Figure 7).

(33) Shoeib, T.; Siu, K. W. M.; Hopkinson, A. C. *J. Phys. Chem. A* **2002**, *106*, 6121.
(34) Van Hyning, D.; Zukoski, C. *Langmuir* **1998**, *14*, 7034.
(35) Stracke, R.; Böhm, K. J.; Wollweber, L.; Tuszynski, J. A.; Unger, E. *Biochem. Biophys. Res. Com.* **2002**, *293*, 602.
(36) Levenson, G.; Twist, P. *J. Photogr. Sci.* **1973**, *21*, 219.

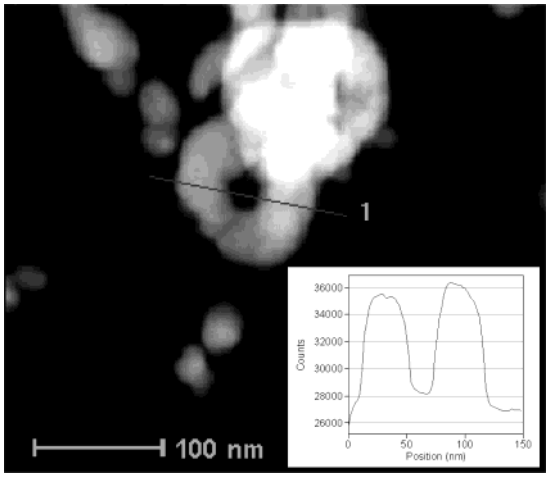

Figure 8. High-angle annular-darkfield (HAAD) scanning transmission electron micrograph displaying a cross section of a silver-metallized microtubule. The inset shows the EDX (Ag $K_{\alpha 1}$) linescan in 1.

In their native state, microtubules (MTs) are highly linear structures. As in the case of sodium borohydride reduction, metallization yielded mainly curved silver/microtubule structures, which implies that the structural integrity of the MTs was not retained during the metallization process. The question arises as to whether the observed metal structures are hollow tubules or solid rods with the biotemplate completely destroyed during the metallization process. Hence, ultrathin sections of the metallized microtubules were produced, showing sections transverse to the long axis of the tubule. Figure 8 displays a cross section of a silver wire, which suggests that the observed silver wires were hollow silver tubules. The inner diameter of the metal tubules is 25 nm, corresponding, in fact, to the outer diameter of the microtubules.

TEM images revealed that the nucleation of some tiny silver seeds preceded the formation of a continuous metal coating, thus providing some activation of the biopolymer (Figure 5A); however, the actual process of seed formation remains unclear. In contrast to the development of microtubules densely packed with preformed 5-nm silver particles, however, the metal coating was not deposited homogeneously over the whole length of the template, but seemed to be initiated at certain points on the outside wall of the biopolymer with a metal film growing heterogeneously along the length of the template. When the reducing agent was added to the template prior to the metal ions, thus preventing any metal incubation of the template, no metal wires were observed. On the basis of these results, we suggest that the interaction of the template with metal ions is important for the formation of the wires and that, after an initial activation of the template, the silver film grows heterogeneously along the outside wall of the microtubule, leading to a selective metallization of the template. In this approach, the biostructure serves as a functionalized scaffold where the metal is generated heterogeneously and shaped into a nanostructure with its morphology dependent on that of the biotemplate.

4. Conclusions

Microtubules, highly oriented protein assemblies with defined surface functionalities, can serve as bioorganic templates for the fabrication of various silver nanomaterials. Depending on the kind of reducing agent and the pH value used, small silver particles could be nucleated and densely bound to the tubular structure of the biotemplate. These particles could be enlarged to grain sizes of 10−30 nm by applying hydroquinone and silver ions. Even completely continuous nanowires could be achieved by using a similar method. One problem, however, concerned the stability of these structures in solution, as they tend to agglomerate into extended networks. There remains a great potential to apply these metallization techniques to other protein assemblies to produce silver/protein composites with interesting material properties.

Acknowledgment. The authors thank Drs. Thomas Stoiber and Tobias Neumann for providing microtubule protein, Katrin Buder for ultrathin cross-sectioning, and Günther Bürkle and Dr. Harald Rösner for assistance with transmission electron microscopy. This work is dedicated to Prof. Eckhard Dinjus on the occasion of his 60th birthday.

CM049462S